

In vitro reconstitution of lateral to end-on conversion of kinetochore–microtubule attachments

Manas Chakraborty², Ekaterina V. Tarasovets, Ekaterina L. Grishchuk¹

Perelman School of Medicine, University of Pennsylvania, Philadelphia, PA, United States

¹*Corresponding author: e-mail address: gekate@penmedicine.upenn.edu*

CHAPTER OUTLINE

1 Introduction	2
1.1 Microtubule End Conversion At the Kinetochores of Mitotic Cells.....	2
1.2 Current Methods for Studying Kinetochore–Microtubule Interactions in Vitro	3
1.3 Rationale for the CENP-E Kinesin-Mediated Microtubule End-Conversion Assays.....	3
2 Materials	5
2.1 Equipment.....	5
2.2 Image Analysis Software	6
2.3 Materials	8
2.4 Reagents	8
2.5 Buffers.....	9
2.6 Protein Preparation.....	10
2.7 Handling of Proteins.....	10
2.8 Preparation of Stabilized MTs.....	11
3 Methods	12
3.1 Assay for Investigation of Interactions Between Kinetochore Proteins and Microtubules During Lateral Gliding	12
3.2 Assay for Investigation of the Transition From Microtubule Lateral to End Binding	15
3.3 Assay for Reconstitution of Dynamic Microtubule End-On Attachment	17
4 Outlook	18
Acknowledgments	19
References	19

²Current address: Centre for Mechanochemical Cell Biology, Warwick Medical School, Coventry, United Kingdom.

Abstract

During mitosis, kinetochores often bind to the walls of spindle microtubules, but these lateral interactions are then converted into a different binding mode in which microtubule plus-ends are embedded at kinetochores, forming dynamic “end-on” attachments. This remarkable configuration allows continuous addition or loss of tubulin subunits from the kinetochore-bound microtubule ends, concomitant with movement of the chromosomes. Here, we describe novel experimental assays for investigating this phenomenon using a well-defined *in vitro* reconstitution system visualized by fluorescence microscopy. Our assays take advantage of the kinetochore kinesin CENP-E, which assists in microtubule end conversion in vertebrate cells. In the experimental setup, CENP-E is conjugated to coverslip-immobilized microbeads coated with selected kinetochore components, creating conditions suitable for microtubule gliding and formation of either static or dynamic end-on microtubule attachment. This system makes it possible to analyze, in a systematic and rigorous manner, the molecular friction generated by the microtubule wall-binding proteins during lateral transport, as well as the ability of these proteins to establish and maintain association with microtubule plus-end, providing unique insights into the specific activities of various kinetochore components.

ABBREVIATIONS

MAP	microtubule-associated protein
MT	microtubule
TIRF	total internal reflection fluorescence

1 INTRODUCTION

1.1 MICROTUBULE END CONVERSION AT THE KINETOCHORES OF MITOTIC CELLS

During vertebrate mitosis, the kinetochores of sister chromatids engage in dynamic interactions with spindle microtubules (MTs), undergoing highly complex motions (McIntosh, Grishchuk, & West, 2002; Rieder & Salmon, 1998; Walczak, Cai, & Khodjakov, 2010). Initially, the kinetochores of most chromosomes form lateral attachments to the walls of spindle MTs, although some may be captured directly by the MT plus-end (Hayden, Bowser, & Rieder, 1990; Magidson et al., 2011; Tanaka et al., 2005). During subsequent congression of the pole-proximal chromosomes, the kinetochore-bound, MT plus end-directed kinesin CENP-E transports chromosomes by moving along the MT walls (Kapoor et al., 2006; Maiato, Gomes, Sousa, & Barisic, 2017; Wood, Sakowicz, Goldstein, & Cleveland, 1997). After chromosomes arrive at the spindle midzone, where the plus-ends of the kinetochore-bound MTs are located, the kinetochores transition from the lateral MT binding to MT end-on attachment (Gudimchuk et al., 2013; Shrestha & Draviam, 2013). In this remarkable configuration, chromosomes move synchronously with MT dynamics as the MT plus-ends tethered by the kinetochore microtubule-associated proteins (MAPs)

undergo continuous de/polymerization (Grishchuk, 2017). Although many, or perhaps all, of the important players in the kinetochore-mediated MT end conversion have been identified, a deep mechanistic understanding of the underlying molecular mechanisms remains elusive.

1.2 CURRENT METHODS FOR STUDYING KINETOCHORE–MICROTUBULE INTERACTIONS IN VITRO

Reconstitution methods have contributed significantly to our understanding of the mechanisms of kinetochore–MT interactions, and have helped to reveal the specific roles played by various kinetochore components. The early *in vitro* work successfully used isolated mammalian chromosomes to demonstrate the presence of ATP-dependent motors of opposite polarity at the kinetochores (Hyman & Mitchison, 1991, 1993; Mitchison & Kirschner, 1985), as well as the ability of kinetochores to move while bound to depolymerizing MT plus-ends even in the absence of ATP (Coue, Lombillo, & McIntosh, 1991). Coverslip-immobilized chromosomes have been used to directly observe de/polymerization of kinetochore-bound MT plus-ends, providing insights into their dynamic behavior (Hunt & McIntosh, 1998; Koshland, Mitchison, & Kirschner, 1988). More recently, purified kinetochore particles from budding yeast have been employed to dissect the roles of molecular components involved in the processive movement of these particles at dynamic MT plus-ends, either freely or under force exerted with laser tweezers (Akiyoshi et al., 2010; Driver, Powers, Sarangapani, Biggins, & Asbury, 2014). Similar motility assays and laser trapping methods were used to characterize MT end-coupling by recombinant kinetochore MAPs conjugated to microbeads (Asbury, Gestaut, Powers, Franck, & Davis, 2006; Grishchuk et al., 2008; Lombillo, Coue, & McIntosh, 1993; McIntosh, Volkov, Ataulakhanov, & Grishchuk, 2010). The latter method is particularly useful for mechanistic studies of the underlying coupling mechanisms and force generation by the MT depolymerization motor (Grishchuk, McIntosh, Molodtsov, & Ataulakhanov, 2012; Volkov et al., 2013). In these assays, however, a bead becomes associated with the dynamic MT plus-end either following depolymerization of the bead–distal MT fragment, as with “segmented” MTs (Grishchuk & Ataulakhanov, 2010), or after the bead is brought into direct contact with the MT plus-end with the help of an optical trap (Driver et al., 2014). Although these approaches allow characterization of the processivity and load bearing of dynamic MT plus-end attachment, they provide no direct insight into the processes by which lateral MT binding is converted into end attachment.

1.3 RATIONALE FOR THE CENP-E KINESIN-MEDIATED MICROTUBULE END-CONVERSION ASSAYS

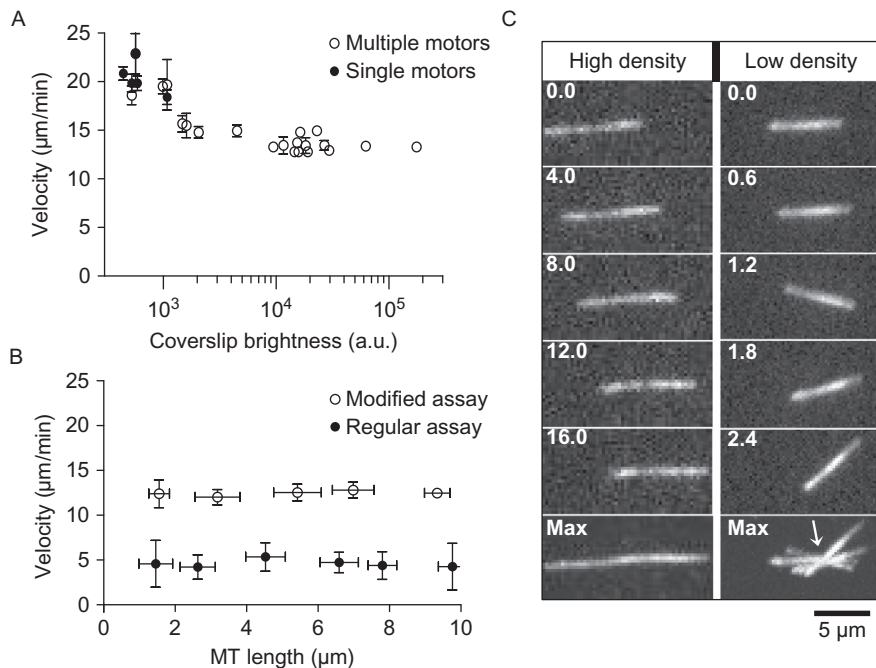
In this chapter, we describe a reductionist approach to examining several aspects of the MT end-conversion phenomenon: the behavior of selected MAPs during their lateral motion along the MT wall, the transition from MT lateral to end

binding, and the ability of this attachment to accommodate continuous addition or loss of tubulin subunits. The main advantage of our novel approach is that it recapitulates the physiological end-conversion pathway involving the plus end-directed CENP-E kinesin. Specifically, we use a recombinant construct derived from *Xenopus laevis* CENP-E, truncated to remove most of its coiled-coil stalk and tail (Kim, Heuser, Waterman, & Cleveland, 2008; Wood et al., 1997). This motor moves on the MT wall similarly to the full-length protein, but detaches readily from MT plus-ends and fails to move in conjunction with MT dynamics because it lacks the MT-binding tail (Gudimchuk et al., 2013). Our assays combine this motor with another MT-binding protein, e.g., a kinetochore MAP. Because both proteins are immobilized on a surface of either the coverslip or the coverslip-bound microbeads, they cannot interact directly, and instead engage in interactions with the MTs, potentially leading to synergistic behaviors due to mechanical coupling.

The first assay we developed using this motor examines motions of the stabilized MTs gliding over a surface containing a mixture of CENP-E and a MAP of interest in the presence of ATP (Figs. 1 and 2). Because MTs move laterally on this surface, while interacting with both the transporting motor and the passively binding MAP, this assay mimics kinetochore transport during CENP-E-driven chromosome congression (Kapoor et al., 2006). A significant decrease in the MT gliding velocity in the presence of a MAP would indicate that MAPs can generate molecular friction on a moving MT, suggesting its involvement in regulating the velocity of congressing chromosomes.

In the second assay (Fig. 3), a mixture of these proteins is conjugated to the surface of coverslip-immobilized microbeads, representing the surface of a simplified kinetochore. The advantage of this geometry is that the CENP-E kinesin glides MT minus-end forward, so that the MT plus-end is the final point of contact between the MT and the kinetochore-representing bead, mirroring the polarity of MT attachment to real kinetochores. Because the truncated CENP-E cannot hold onto the MT plus-ends, any effects on the establishment and the maintenance of binding between the bead and the MT plus-end can be attributed to the activity of the MAP, coupled mechanically to the CENP-E through the MT. Thus, examining the behavior of an MT that has reached its terminal contact should provide valuable insights into the ability of kinetochore MAPs to support the MT wall-to-end transition.

The last assay incorporates soluble tubulin into this system, and can therefore probe the ability of the bead-attached MT plus-ends to add and lose tubulin subunits without loss of bead attachment. The dynamics of kinetochore-bound MT ends in dividing cells, as well as of MT ends coupled to the kinetochores of isolated chromosomes, are altered relative to MT plus-ends that are not kinetochore-bound (Akiyoshi et al., 2010; Hunt & McIntosh, 1998), consistent with the existence of a kinetochore “governor” (Nicklas, 1983). Thus, this assay should facilitate the identification and mechanistic analysis of the molecular components that underlie properties of the still-elusive governor.

**FIG. 1**

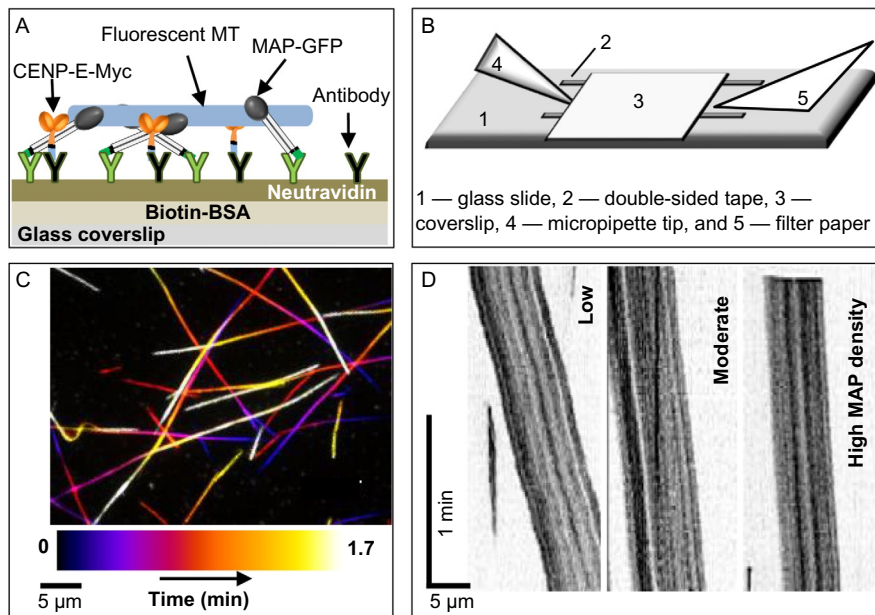
Gliding assay with CENP-E motor. (A) Velocity of MT gliding (mean \pm SEM) as a function of coverslip brightness, measured via GFP fluorescence. Coverslip was coated with truncated CENP-E-GFP according to steps 1–7 in Section 3.1. CENP-E-GFP density was varied by using different concentrations of anti-GFP antibody and excess soluble CENP-E-GFP motor. *Open* and *filled circles* correspond to the translational velocities of linearly gliding MTs and pivoting MTs, respectively. (B) MT gliding velocity vs MT length (mean \pm SD) in experiments using our “modified” assay described in Section 3.1 or a “regular” gliding protocol in which CENP-E motors and antibodies were adsorbed on the coverslip lacking the BSA-neutravidin coating. (C) Representative images of two MTs moving over coverslips with either high ($>10^3$ a.u.) or low ($<10^3$ a.u.) motor densities. *Numbers* indicate imaging time (in seconds). *Bottom images* show maximum intensity projections, illustrating predominantly linear motion (*left*) or translocation with pivoting around a fixed point (*arrow*), indicative of a single motor interaction.

2 MATERIALS

2.1 EQUIPMENT

The dynamics of MT plus-ends or lateral MT gliding are best recorded using fluorescently labeled MTs and total internal reflection fluorescence (TIRF) microscopy. However, because the evanescent field decays rapidly with distance from the coverslip, imaging deeper into the microscopy chamber requires adjustment of the TIRF angle or the use of regular epifluorescence illumination. Accordingly, our experimental setup

6 Kinetochore–microtubule attachments

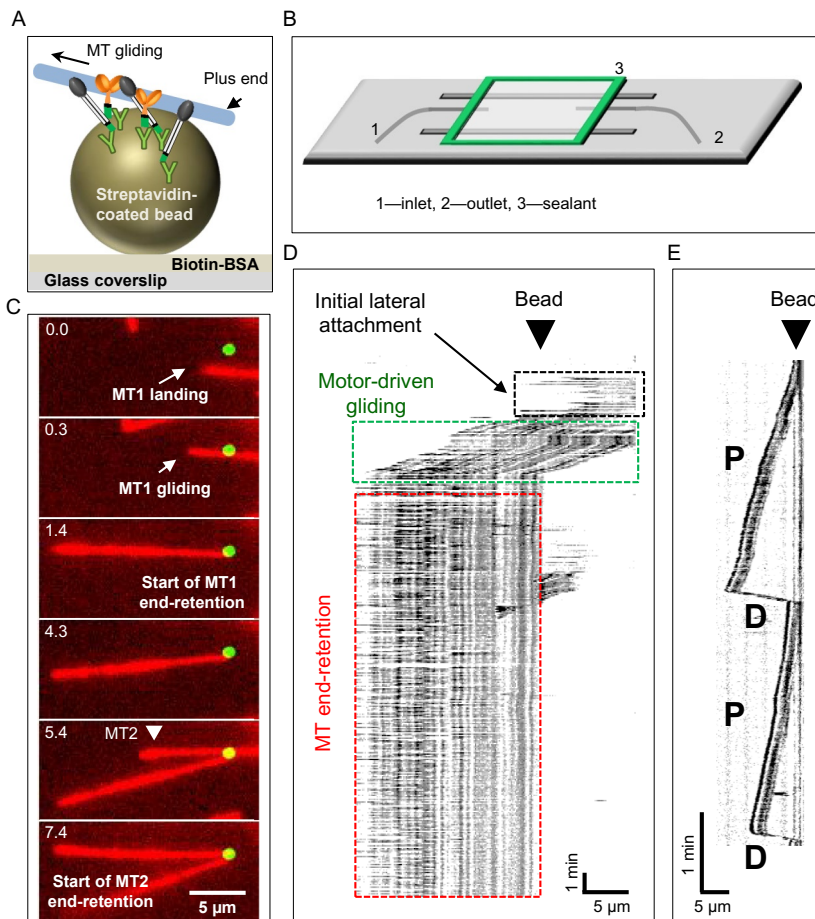
**FIG. 2**

Interactions between a kinetochore MAP and the walls of the CENP-E-transported microtubules. (A) Schematic representation of the MT gliding assay using truncated CENP-E-Myc and a kinetochore MAP tagged with GFP. Proteins were immobilized on the coverslip with anti-Myc and anti-GFP antibodies, shown as *black* and *green* Ys, respectively. (B) Schematic of perfusion through the flow chamber used in this assay. (C) Maximum projection of a 100-frame time series of gliding MTs acquired at 1 frame/s. Colors represent different times, as indicated by the *color-coded scale* below. (D) Representative kymographs of three MTs gliding on surfaces coated with CENP-E and a kinetochore MAP (Ndc80 protein complex) at different surface densities.

uses a Nikon Eclipse Ti microscope equipped with 1.49NA TIRF 100× Oil objective and laser illumination that can be used in either TIRF or in epifluorescence modes. A coherent CUBE 640-nm diode laser provides excitation for MTs polymerized from HiLyte647-labeled tubulin, while an analogous 488-nm laser is used to visualize proteins labeled with GFP. Images are acquired on an Andor iXon3 EMCCD camera. The specimen is maintained at 32°C to prevent excessive MT breakdown.

2.2 IMAGE ANALYSIS SOFTWARE

Several commercial or freely available software programs are suitable for tracking the coordinates of MT ends and performing general fluorescence quantification. For these purposes, we routinely use MetaMorph Microscopy Automation and Image Analysis Software (Molecular Devices) and ImageJ (National Institutes of Health, Bethesda, MD).

**FIG. 3**

Transition from lateral to end microtubule binding and coupling at the dynamic microtubule plus-end. (A) Schematic representation of the end-conversion assay (not to scale), in which stabilized MTs glide on the surface of coverslip-immobilized beads. (B) Schematics of perfusion through the reusable flow chamber used in this assay. (C) Selected images of taxol-stabilized MTs (*red*) gliding over beads (*green*) coated with CENP-E kinesin and kinetochore MAP. The *number at the top left corner of each frame* indicates the acquisition time (in minutes) of that frame. Landing of a second MT is marked by *white triangle*. (D) Representative kymograph of a MT obtained with beads coated with CENP-E kinesin and a kinetochore MAP. The MT glides then stays attached to the bead at the MT plus-end. (E) Kymograph of the fluorescent MT seed repeatedly moving away from and back to the bead as MT polymerizes (P) and depolymerizes (D) in the presence of soluble unlabeled tubulin.

2.3 MATERIALS

- Glass coverslips (VWR, cat # 48366-067). To reduce fluorescent background from nonspecific proteins adhered to the surface, coverslips should be cleaned and silanized, e.g., using protocols in (Volkov, Zaytsev, & Grishchuk, 2014).
- Glass slides (VWR, cat # 48312-004). Slide silanization is not required for these assays.
- Double-sided tape (Scotch, cat # 504829).
- Kwik-Cast Sealant (World Precision Instruments, cat # KWIK-CAST).
- Reusable flow chambers with tubing (Volkov et al., 2014).
- Streptavidin-coated polystyrene beads, 0.9 μm diameter (Spherotech, cat # SVP-08-10). These beads can be stored at 4°C for several months without significant loss of activity.

2.4 REAGENTS

Unless otherwise noted, reagents are prepared as stocks in Mg-BRB80 buffer (see below), aliquoted, frozen in liquid nitrogen, and stored at -80°C .

- AMP-PNP (ROCHE, cat # 10102547001) is prepared as a 50mM solution and stored as 5- μL aliquots.
- Biotin-BSA (Sigma-Aldrich, cat # A8549) is prepared at 225 μM and stored as 10- μL aliquots.
- Biotin-PEG (Quanta BioDesign, cat # 10776) is prepared at 40mM and stored as 5- μL aliquots. After thawing, this reagent can be diluted 10-fold in Mg-BRB80 and stored at 4°C for several days without significant loss of blocking activity.
- Biotinylated anti-GFP antibody (Abcam, cat # ab6658) and biotinylated anti-Myc antibody (Millipore, cat # 16170) are prepared at 0.5 mg/mL in 50% glycerol and stored as 30- μL aliquots at -20°C .
- BSA (Sigma-Aldrich, cat # A7638) is prepared at 100 mg/mL and stored as 100- μL aliquots.
- Catalase (Sigma-Aldrich, cat # C40) is prepared at 8 mg/mL and stored as 10- μL aliquots.
- DTT (Thermo Fisher Scientific, cat # 15508) is prepared at 1 M in Milli-Q water, filter sterilized, and stored as 10- μL aliquots.
- EGTA (Sigma-Aldrich, cat # E4378) is prepared at 0.2 M in Milli-Q water, pH is adjusted to 8.0 with NaOH or KOH. The solution is filter sterilized and stored as 10-mL aliquots at -20°C .
- Glucose (Sigma-Aldrich, cat # G8270) is prepared at 600 mg/mL in Milli-Q water and stored as 10- μL aliquots.
- Glucose oxidase (Sigma-Aldrich, cat # G2133) is prepared at 10 mg/mL and stored as 10- μL aliquots.
- Glycerol UltraPure (Invitrogen, cat # 15514011) is aliquoted in 1–10-mL tubes and stored at room temperature.

- GMPCPP (10mM solution, Jena Biosciences, cat # NU-405) is stored as 3.5- μ L aliquots.
- Mg-ATP (Sigma-Aldrich, cat # A9187) is prepared at 100mM and stored as 10- μ L aliquots.
- $MgCl_2$ (Thermo Fisher Scientific, cat # M33-500) is prepared at 1M in Milli-Q water, filter sterilized, and stored as 1-10-mL aliquots at $-20^\circ C$.
- GTP (Sigma-Aldrich, cat # G8877) is prepared at 50mM in 50mM $MgCl_2$, pH adjusted to 7.0 with NaOH, and stored as 10- μ L aliquots.
- Neutravidin (Thermo Fisher Scientific, cat # 31000) is prepared at 50 μ M and stored as 10- μ L aliquots.
- Paclitaxel (taxol) (Sigma-Aldrich, cat # T7402) is prepared at 1mM in DMSO and stored as 10- μ L aliquots.
- PIPES (Sigma-Aldrich, cat #1851) is prepared at 0.5M in Milli-Q water and pH is adjusted to 6.9 with KOH. The solution is filter sterilized and stored at room temperature for several months or at $-20^\circ C$ as 10-50mL aliquots.
- Pluronic F-127 (Sigma-Aldrich, cat # P2443) is prepared as a 1% solution in Mg-BRB80. To dissolve, the solution is incubated on a rocker overnight at room temperature, then heated to $50^\circ C$ for 20min. Aggregates are removed by centrifugation at $16,000 \times g$ for 15min or by passing through a 0.2- μ m filter. Stored at room temperature no longer than 1 week.

2.5 BUFFERS

- Mg-BRB80: 80mM PIPES, 4mM $MgCl_2$, 1mM EGTA buffer is prepared in advance in batches of 50mL or more using original reagents or stock solutions of 0.5M PIPES, 1M $MgCl_2$, and 0.2M EGTA. After pH is adjusted to 6.9 with KOH, the buffer is filter sterilized, aliquoted in suitable vials, and stored at room temperature for several weeks, or at $4^\circ C$ and $-20^\circ C$ for longer periods.

The following buffers are prepared using Mg-BRB80 immediately prior to each experiment. Some reagents, such as DTT and the oxygen-scavenging system, are not stable; accordingly, these buffers should be prepared fresh every 4-5h.

- Wash buffer: Mg-BRB80 supplemented with 2mM DTT and 4mg/mL BSA. ATP-containing Wash buffer is prepared with 0.1mM Mg-ATP; the AMP-PNP-containing Wash buffer is prepared with 0.1mM AMP-PNP.
- Image buffer: Mg-BRB80 supplemented with 10mM DTT, 4mg/mL BSA, 0.1mg/mL glucose oxidase, 80 μ g/mL catalase, and 6mg/mL glucose.
- Motility Image buffer: Image buffer supplemented with 2mM Mg-ATP and 10 μ M taxol. Taxol should be omitted when GMPCPP-containing MTs are used, and 1mM GTP should be added when soluble tubulin is used to elongate the GMPCPP-containing MT seeds.

2.6 PROTEIN PREPARATION

- Tubulin: Bovine or porcine tubulins can be purchased from commercial sources (e.g., Cytoskeleton, Inc.) or purified according to published protocols. We purify tubulin from cow brains using two thermal cycles of polymerization and depolymerization, phosphocellulose chromatography, and two additional thermal cycles to produce highly competent and MAP-free tubulin preparation (Miller & Wilson, 2010). Final tubulin concentration is adjusted to 10 mg/mL in Mg-BRB80; 5–10- μ L aliquots are frozen in liquid nitrogen and stored at -80°C . Fluorescent tubulin is prepared by labeling these preparations with amine-reactive dyes as in Hyman et al. (1991). We employ HiLyte Fluor 647 acid NHS ester (AnaSpec, cat # 81256), achieving a labeling efficiency of 0.2–0.5. Labeled tubulin is stored at -80°C in 3–5- μ L aliquots, or as needed.
- Kinesin CENP-E: The truncated *X. laevis* CENP-E construct (aa 1–473) contains only the motor domain, neck linker, and a segment of the coiled-coil stalk that is sufficient for dimerization. Truncated CENP-E constructs fused at the C-terminus to either GFP-6xHis or Myc-6xHis are expressed in *E. coli* and purified as described in Kim et al. (2008) and Wood et al. (1997). CENP-E protein stocks (0.5 μM) are supplemented with 25% glycerol and stored at -80°C as 40- μ L aliquots.
- Kinetochore MAPs: Our assays are designed to probe the roles of different MAPs, which should be prepared according to their individual purification protocols.

2.7 HANDLING OF PROTEINS

- Protein aliquots are thawed briefly on ice immediately prior to their use in the assays. Tubulin aliquots are spun briefly, and the supernatants are used immediately to polymerize MTs because prolonged storage of tubulin may cause it to aggregate.
- After a kinetochore MAP is thawed and diluted to the desired concentration (typically 0.1 μM), protein aggregates are removed by ultracentrifugation at $140,000 \times g$ for 30 min at 4°C . Supernatant is immediately collected and kept on ice for the duration of the assay. Because the extent of protein aggregation varies among protein preparations, this procedure often decreases the soluble protein concentration. Therefore, the final MAP concentration should be determined by conventional methods, such as the Bradford assay (Sigma-Aldrich, cat # B6916), or by the fluorescence-based microscopy approach described immediately below.
- The soluble concentration of a GFP-labeled protein can be determined by measuring its fluorescence in a microscopy chamber. This method is particularly useful when working with limited amounts of protein because it requires significantly less protein than conventional assays. First, the concentration of any other aggregate-free GFP-protein available in nonlimiting quantities is determined by the Bradford assay or spectrophotometry (extinction coefficient

for GFP at 488 nm is $55,000 \text{ M}^{-1} \text{ cm}^{-1}$ (Tsien, 1998)). Serial dilutions of this “standard” protein in the range of 0.5 nM to 0.5 μM are then prepared in Image buffer containing antibleaching agents and BSA, and added to a flow chamber prepared as instructed in step 1 of Section 3.1 and preblocked with 1% Pluronic. Images should be collected immediately after adding the GFP-protein solutions, in order of increasing concentration. Timing is important because upon extended incubation, a significant fraction of the protein may adsorb to the glass surfaces of the chamber, especially when the protein concentration is low or blocking reagents such as BSA are absent. Alternatively, the GFP-protein can be flowed into the chamber continuously using a pump, as in Volkov et al. (2014), so that soluble protein is not depleted. To avoid measuring fluorescence from the coverslip-adsorbed protein, images are acquired in epifluorescence mode some distance (e.g., 10 μm) away from the coverslip. Images of 10–15 different fields are collected, making sure that the field diaphragm is minimally opened, and the illumination shutter remains open only during the acquisitions. Mean GFP fluorescence intensities of the central quadrants of these images are averaged to plot a calibration curve of GFP fluorescence vs soluble protein concentration (calculated based on the results of a conventional assay and known dilution factors). The intensity of the same region recorded with a closed shutter should be subtracted in case camera noise is significant. In a linear regime of EMCCD operation, the resultant calibration curve should fit a straight line intercepting the graph’s origin. For our instrument, we use 100% power of 488-nm laser, exposure time of 300 ms, $5 \times$ conversion gain, 1 MHz readout speed, and 16-bit sensor mode for Andor iXon3 EMCCD. To avoid saturating the EMCCD at higher protein concentrations, either the laser power or exposure time can be reduced, but it should be confirmed via independent measurements that image intensity is a linear function of these parameters. The calibration curve is subsequently used to estimate the concentrations of the GFP-labeled proteins used in the motility assays.

2.8 PREPARATION OF STABILIZED MTs

To prepare taxol-stabilized MTs, mix labeled and unlabeled tubulin in the desired ratio to achieve either speckled or even MT labeling. Our typical mix is prepared with 7.5 μL of unlabeled tubulin (10–12 mg/mL) and 3 μL fluorescent tubulin (4–6 mg/mL; degree of labeling 0.2–0.5). Add 4 μL glycerol and 1.5 μL GTP (diluted from stock to 10 mM with Mg-BRB80), mix well by pipetting, and immediately place in a 37°C water bath for 20 min. Incubation time can be increased to yield longer MTs. Add 1.8 μL of 0.1 mM taxol (diluted in Mg-BRB80 and warmed to 37°C), mix well without removing from the water bath, and incubate for an additional 10 min. Add 100 μL of warm Mg-BRB80 buffer supplemented with 10 μM taxol, and pellet MTs by spinning at room temperature in an Eppendorf centrifuge at $16,000 \times g$ for 15 min. To increase yield, centrifuge in an AirFuge (Beckman Coulter, rotor A-100/18) at $66,000 \times g$ for 3 min. Remove the supernatant, wash

the pellet by gently adding, then remove 100 μL of warm Mg-BRB80 buffer supplemented with 10 μM taxol, thoroughly resuspend the pellet in 50 μL of the same buffer. To avoid fragmenting the MTs, use a cutoff pipette tip and minimize pipetting time. Store MTs in the dark at 20–25°C for no more than 3 days. To prepare GMPCPP-containing MTs or short MT fragments (seeds), follow the protocol in Volkov et al. (2014) using fluorescently labeled tubulin, and store these MTs in Mg-BRB80 with 1 mM GMPCPP.

3 METHODS

3.1 ASSAY FOR INVESTIGATION OF INTERACTIONS BETWEEN KINETOCHORE PROTEINS AND MICROTUBULES DURING LATERAL GLIDING

Gliding assays have been used extensively to study the motile behavior of cytoskeletal motors and their ability to propel movement of MTs or actin filaments in an ATP-dependent manner. In a MT gliding assay, taxol-stabilized or GMPCPP-containing MTs are observed as they move on a layer of kinesin (or dynein) motors immobilized on a coverslip surface (Howard & Hyman, 1993; Paschal & Vallee, 1993). For this approach to be successful with CENP-E kinesin, it is essential to optimize preparation of such layers, preserving full activity of the immobilized motor and eliminating nonspecific interactions between the MTs and coverslip that could retard gliding. To this end, in our assay we use antibody-immobilized CENP-E and minimize nonspecific friction from coverslip surface by using BSA-neutravidin coating and selected blocking reagents, as specified below. Under these conditions, the MT gliding velocity is independent of MT length and CENP-E motor density in a wide range (Fig. 1A and B). Using GFP-labeled *X. laevis* CENP-E construct (aa 1–473) we routinely obtain gliding velocities of 14–16 $\mu\text{m}/\text{min}$. This is considerably higher than achieved using a protocol with less surface blocking (Fig. 1B), likely explaining the discrepancy with other CENP-E studies (Espeut et al., 2008). However, the CENP-E gliding velocity we obtain is still somewhat smaller than that reported for single motor molecules assayed under similar conditions, 18–21 $\mu\text{m}/\text{min}$ (Gudimchuk et al., 2013; Yardimci, Duffelen, Mao, Rosenfeld, & Selvin, 2008). We attribute this difference to retardation caused by mechanical coupling of multiple CENP-E motors in the gliding assay (Bieling, Telley, Piehler, & Surrey, 2008). Indeed, when we decreased the CENP-E-coating density by titrating down the antibody concentration, the gliding velocity increased. Under these conditions, some MTs pivoted while gliding (Fig. 1C), indicating the single-molecule regime (Hunt & Howard, 1993). The linear translocation velocities of the pivoting MTs in the gliding assay (Fig. 1A, filled circles) were comparable to the range observed for the motility of single CENP-E-GFP molecules walking along MT walls (Gudimchuk et al., 2013). Interestingly, decreasing the CENP-E coating density by titrating down CENP-E rather than antibody concentration strongly

decreased the MT gliding velocity, apparently due to nonspecific microtubule interactions with the antibodies, further demonstrating the importance of proper coverslip functionalization. When conditions are optimal, this assay can be used to examine how various MAPs interact with the MT wall during its lateral CENP-E-driven motion (Fig. 2A), as described immediately below.

Thaw aliquots with reagent stocks on ice for 10 min, tap-spin to sediment liquids, and keep on ice for the duration of the experiment. Prepare fresh Wash buffer. Dilute reagents to the required concentrations: 22.5 μ M biotin-BSA in Mg-BRB80; 25 μ M neutravidin in Mg-BRB80; 20 μ g/mL biotinylated antibodies in Wash buffer; and 100 μ M biotin-PEG in Mg-BRB80. Prepare ATP-containing Wash buffer by adding Mg-ATP to 0.1 mM. Keep all buffers and reagents on ice until needed.

1. Attach a silanized coverslip over a regular glass slide using spacers made from two strips of a double-sided tape, generating a \sim 15- μ L flow chamber. Place the chamber horizontally over a flat surface and exchange solutions within the chamber using a micropipette and filter paper, as shown in Fig. 2B. Alternatively, gentle exchange of solutions can be achieved by slightly elevating one side of the glass slide and letting the liquid flow by gravity. To facilitate the flow, thin wells can be “painted” using sealant at the entry and exit sides of the chamber (as in Lombillo et al., 1993), preventing the solutions from spreading all over the slide surface. Pump-driven reusable flow chambers can also be used to avoid chamber drying and more precisely control the perfusion rates (Fig. 3A). All incubation steps are done at room temperature except when working with the MTs, when the temperature should be kept at 30–32°C. To avoid drying of the chamber during prolonged incubations, place the chamber in a container or a Petri dish lined with a piece of Kimwipe or filter paper moistened with Milli-Q water.
2. Functionalize the coverslip by perfusing 30 μ L of 22.5 μ M biotin-BSA, incubate for 10 min. For this and subsequent steps, after each incubation wash chamber by perfusing 30 μ L Mg-BRB80 three times. Short 2–5-min incubations between each perfusion tend to improve the reproducibility of the resultant layers.
3. Perfuse 30 μ L of 25 μ M neutravidin, forming a layer of neutravidin molecules attached to the coverslip via biotin-BSA. Incubate and wash as in step 2.
4. Perfuse 30 μ L of 20 μ g/mL biotinylated antibodies (individual or mixed). The choice of antibodies depends on the availability of tagged protein constructs, and will also dictate subsequent options for quantification of the resultant protein density. A mixture of GFP-tagged proteins, e.g., CENP-E and a MAP, can be immobilized via biotinylated anti-GFP antibodies, but in such a case it will not be possible to verify the individual protein binding densities. Alternatively, proteins can be conjugated to anti-GFP antibodies sequentially, verifying their recruitment after each incubation step via increased GFP fluorescence. Finally, a mixture of the anti-GFP antibodies and antibodies against a different tag can be used, as described below, so that only one of the proteins is fluorescent and its conjugation density can be unambiguously

determined. The required antibody concentration should be optimized in advance of these assays, because some antibodies can cause nonspecific retardation of MT gliding, and the extent of this artifact may depend on antibody occupancy by tagged proteins.

5. After the biotinylated antibodies are removed with Wash buffer, block unreacted neutravidin in the chambers by adding biotin-PEG diluted to 100 μM in Mg-BRB80 for 15 min. Biotin-BSA (22.5 μM) can also be used, but it appears to be less efficient than biotin-PEG. Wash the chamber as in step 2 using Mg-BRB80 buffer.
6. Block exposed silanized glass surface by perfusing 30 μL of 1% Pluronic. Incubate for 10 min and wash as in step 2, using ATP-containing Wash buffer.
7. Flow in 30 μL of freshly diluted truncated CENP-E-Myc (0.1 μM in ATP-containing Wash buffer), incubate for 30 min, and wash as in step 2 using ATP-containing Wash buffer. Because the velocity of MT gliding by CENP-E is independent of its density within a wide range, it is not necessary to accurately monitor the density of this motor.
8. Flow in the GFP-tagged kinetochore protein under study (30 μL in ATP-containing Wash buffer), incubate for 30 min, and wash as above. To obtain different surface densities of the protein, vary its concentration among chambers (suggested range: 10–200 nM).
9. During the incubation in step 8, prepare 400 μL of Motility Image buffer and keep at 32°C. For optimal activity of the oxygen-scavenging system, the buffer should be made fresh just before imaging. After the incubation in step 8 is completed, wash the chamber twice with 30 μL of ATP-containing Wash buffer, followed by 30 μL of prewarmed Motility Image buffer.
10. To preserve MT integrity and decrease background from MT fragments, all subsequent steps and solutions should be kept at 32–37°C. Use 60 μL of Motility Image buffer to prepare a fresh dilution of the taxol-stabilized or GMPCPP-containing MTs labeled with HiLyte647. MT concentration should be optimized in separate experiments; for consistency, proper MT concentration should be verified for each preparation by visually inspecting the MT solutions in a separate “wet mount” chamber prepared with no tape spacers (3–4 μL volume).
11. Wash 30 μL of the MT solution into the flow chamber containing the conjugated proteins, and seal the chamber with Kwik-Cast sealant to prevent drying during extended image acquisitions. Immediately place the slide on a prewarmed microscope stage (32°C), focus, and acquire time series for 10–20 min. MT motion should start immediately and will continue for at least 1 h. Regular epifluorescence can be used, but the images usually look more crisp in the TIRF mode. Typical instrument settings for our system are as follows: 5%–15% power for the 640-nm laser, and 100–300 ms exposure, 5 \times conversion gain, 1 MHz readout speed, and 16-bit sensor mode on the Andor iXon3 EMCCD camera. Images are collected at 1 frame/s for 5–10 min for 2–4 image fields.

12. After acquiring MT images, switch to the GFP channel and acquire images of the coverslip surface using epifluorescence, which produces more even field illumination than TIRF. To minimize unnecessary photobleaching, keep the field diaphragm minimally opened to illuminate only the area imaged by the camera, reduce light source intensity, and minimize exposure time. Collect images of 10–15 different fields, keeping the shutter closed when changing between fields.

To determine MT gliding velocities, analyze image sequences by creating maximum image projections (Fig. 2C) and use the resulting trajectories to build kymographs (Fig. 2D) for about 30 MTs from several fields. To examine the frictional resistance of different MAPs, plot MT gliding velocities as a function of GFP brightness of the coverslip, which reflects the density of the coverslip-conjugated MAPs.

3.2 ASSAY FOR INVESTIGATION OF THE TRANSITION FROM MICROTUBULE LATERAL TO END BINDING

In this assay, MTs glide on the surface of beads coated with a mixture of two proteins: the truncated CENP-E motor and a kinetochore MAP (Fig. 3A). The protocol for creating bead coats is similar to that described in Section 3.1 for the coverslip surfaces. However, to increase the number of MTs per image field, MTs are initially attached to the protein-coated beads in presence of a low concentration of the non-hydrolyzable ATP analog AMP-PNP, which prohibits CENP-E gliding. MT gliding is then triggered by addition of a buffer containing Mg-ATP. Alternatively, imaging can be performed using only the buffer with Mg-ATP, as in the regular gliding assay, but the MTs will glide as soon as they land on the beads.

1. Thaw and prepare all reagents, and make dilutions of biotin-BSA, biotin-PEG, and biotinylated antibodies as described in Section 3.1. Prepare AMP-PNP-containing Wash buffer, and keep on ice until needed. Prepare 50- μ L solutions of streptavidin-coated polystyrene beads by washing 1 μ L of bead stock in 150 μ L of Mg-BRB80 (centrifuge at $8000 \times g$ for 6 min). Resuspend beads in 50 μ L of Wash buffer, vortex for 30s, and keep on ice until step 6.
2. Take a dry reusable flow chamber with tubing (Volkov et al., 2014). Attach a silanized glass coverslip to the imaging side of the flow chamber using double-sided tape. Seal the chamber by applying Kwik-Cast sealant around the edges of the coverslip (Fig. 3B).
3. To perfuse solutions into the flow chamber, insert the inlet tubing into a 0.5-mL Eppendorf tube containing the required solution. Connect the outlet tube to a peristaltic pump (e.g., Watson-Marlow, cat # 403U/VM2) and draw the liquid at 5–20 μ L/min.
4. Perfuse 30 μ L of 22.5 μ M biotin-BSA and incubate for 10 min. Wash the chamber by perfusing 100 μ L of Mg-BRB80.
5. Perfuse 30 μ L of 1% Pluronic solution and incubate for 10 min. Wash the chamber by perfusing 100 μ L of Mg-BRB80.

6. Sonicate prepared bead solution in an ultrasonic bath in ice water for 45 s to dislodge any bead clumps. Immediately perfuse bead solution into the chamber and incubate for 10 min. Wash the chamber by perfusing 100 μ L of Mg-BRB80.
7. Perfuse 30 μ L of 20 μ g/mL biotinylated anti-GFP antibody in Wash buffer, incubate for 15 min, and wash the chamber by perfusing 100 μ L of Wash buffer.
8. Perfuse 30 μ L of 100 μ M biotin-PEG, incubate for 10 min, and wash by perfusing 100 μ L of Wash buffer. During this incubation, prepare fresh Image buffer and Motility Image buffer.
9. Perfuse 30 μ L of 0.1 μ M truncated CENP-E-GFP freshly prepared in Wash buffer, incubate for 30 min, and wash the chamber twice with 30 μ L of Wash buffer, then once with the Image buffer.
10. Place the flow chamber on a microscope stage prewarmed to 32°C. Take several images of beads in the GFP channel using epifluorescence illumination. With our instrument, we use 5% power for the 488-nm laser and same Andor iXon3 EMCCD settings as in step 11 in [Section 3.1](#). Save images for subsequent analysis of the GFP brightness of the beads, which corresponds to the density of CENP-E bead coating. For all subsequent steps, use buffers and solutions prewarmed to 32–37°C.
11. Wash the chamber once with Wash buffer, then perfuse 30 μ L of 0.1 μ M solution of the GFP-labeled MAP under study, freshly prepared in Wash buffer. Incubate for 30 min, wash the chamber as in step 9, and acquire images as in step 10. The increase in the GFP brightness of the beads relative to the brightness measured at step 10 reflects the density of MAP coating.
12. Perfuse 30 μ L of HiLyte647-labeled taxol-stabilized MTs in warm AMP-PNP-containing Wash buffer supplemented with 10 μ M taxol, and incubate for 10 min. Perfuse 30 μ L of the same buffer at 5 μ L/min to remove any unbound MTs. Taxol should be omitted when GMPCPP-containing MTs are used. Start image acquisition in epifluorescence mode while perfusing 30 μ L of warm Motility Image buffer containing ATP: most of the bead-bound MTs should initiate gliding within minutes after the start of perfusion. TIRF imaging is not recommended because under regular TIRF illumination, only the bottom parts of the coverslip-attached beads (diameter 0.9 μ m) can be imaged. Most of the bead-bound MTs are not visible in TIRF because they are located hundreds of nanometers away from the coverslip. Recommended instrument settings are 50% power for the 640-nm laser, and 100 ms exposure, 5 \times conversion gain, 10 MHz readout speed, 14-bit sensor mode, and 200 EM gain on Andor iXon3 EMCCD. Acquire images at 15 frames/min for 30 min or until MTs bleach completely.

To analyze these results, select MTs that glided on bead's surface until their trailing ends reached the bead ([Fig. 3C](#)) and build kymographs to identify the gliding phase and the duration of the MT end-retention phase ([Fig. 3D](#)). Bead brightness can be determined as integral intensity of the 3.5 μ m \times 3.5 μ m area surrounding the bead minus the intensity of the same area at a nearby location. The output parameters

of this assay—the fraction of the MTs that exhibited end-retention and the end-retention time for different protein coats—reflect the ability of a given MAP to establish and maintain the MT plus-end attachment.

3.3 ASSAY FOR RECONSTITUTION OF DYNAMIC MICROTUBULE END-ON ATTACHMENT

In the previous section, we described an assay for studying MT wall-to-end transition using stabilized MTs. In real cells, however, the end-on-bound kinetochore MT is dynamically coupled, i.e., it is constantly remodeled by the addition or loss of tubulin subunits at the attachment site. To reconstitute dynamic MT end-coupling, here we modify the protocol in [Section 3.2](#) to include soluble tubulin after the bead-bound proteins have already formed the end-on attachment. Short GMPCPP-containing MT fragments are used due to their ability to serve as “seeds” for MT elongation in the presence of soluble tubulin. The MT seeds are made fluorescent to allow visualization of their gliding on bead surfaces and subsequent motions driven by the MT plus-end dynamics. Because imaging is carried out in the epifluorescence mode, unlabeled or dimly labeled soluble tubulin should be used to decrease background fluorescence. Although the MT elongates at both ends, the brightly labeled seeds used in this protocol serve as fiducial markers that enable unambiguous determination of the segments that polymerize specifically at the bead-attached MT plus-ends.

1. Follow protocol in [Section 3.2](#) using GMPCPP-containing MT seeds labeled with HiLyte647 or a similar dye. Confirm that MT gliding has commenced and most of the MTs become attached to beads at their ends.
2. Thaw an aliquot of tubulin and prepare 30 μL of soluble unlabeled or dimly labeled tubulin (final concentration 0.6 mg/mL) in Motility Image buffer with no taxol, and supplemented with 1 mM GTP.
3. Immediately after preparing the tubulin solution, warm the tube by incubating at 32–37°C for 30 s and perfuse into chamber at 5 $\mu\text{L}/\text{min}$. Increase image acquisition rate to 1 frame/s and record motions until all MTs detach or bleach completely. Upon addition of tubulin, successful MT end-coupling will be evident from the periodic motion of bright MT seeds away from and back to the bead where their unlabeled ends are tethered ([Fig. 3E](#)).

To analyze these images, identify bright MT segments that underwent gliding on the beads and subsequent periodic motions. When interpreting these motions, it is important to keep in mind that the motion of the bright MT segment away from the bead can also be caused by CENP-E-dependent transport along the unlabeled part of the polymerizing MTs, not just by the polymerization at the bead-attached MT plus-end. However, because the seed’s motion back to the bead can only be explained by the MT depolymerization, periodic motions that have both “away” and “back” phases are likely to reflect the dynamics of bead-attached MT plus-ends rather than CENP-E-dependent transport. These de/polymerization rates and

transition frequencies can be measured directly from image sequences or with the help of kymographs, as in Fig. 3E. Other parameters, such as the dynamic attachment time (the total time that a bead-tethered MT seed is observed moving) and the distribution of MT lengths at the time of catastrophe (abrupt switch into depolymerization of the bead-attached MT end), should further aid in comparing the abilities of different kinetochore proteins to sustain MT end-coupling and modify dynamics of the coupled MT plus-end.

4 OUTLOOK

In this chapter, we describe assays that can be routinely used to investigate the abilities of various kinetochore MAPs to mediate MT end conversion promoted by kinetochore kinesin CENP-E. Our overall approach is inspired by the known ability of molecular ensembles comprising the ATP-dependent motor domains and nonmotor MAPs to exhibit emergent behaviors (e.g., Braun et al., 2017; Gudimchuk et al., 2013). Understanding of these complex behaviors requires theoretical modeling based on experimental parameters, and the reconstructed *in vitro* system described here represents a powerful method for obtaining such quantitative characteristics. Our assays build on the well-known MT gliding system and are straightforward to use, requiring only standard reagents and conventional fluorescence microscopy. The advantage of using protein-coated beads, which serve as surrogate kinetochores, that are immobilized on the coverslip rather than floating in solution is that a significantly larger number of end-conversion events can be observed per field during one experimental session. Moreover, thermal noise at MT-coupled sites on immobilized beads is reduced, improving quality of imaging. Solutions can be readily exchanged without disturbing bead positions, allowing the researcher to easily control the composition of the bead coats and molecular milieu. By taking advantage of the natural CENP-E-dependent pathway for the formation of MT attachments, this system provides consistent and well-defined geometry corresponding to the real physiological arrangement. Finally, this system excludes the possibility that MAP-coated beads will roll on the MT surface during coupling of dynamic MT ends, thereby avoiding the associated artifacts (Grishchuk & Ataullakhanov, 2010; Grishchuk et al., 2008). We envision that these assays will be useful in future experiments of increasing molecular complexities, employing multiple kinetochore proteins. This system should also permit application of forces to the MT-coupled end via introduction of an additional bead “handle” at the MT minus-end, as employed in Hunt and McIntosh (1998). Increasing the separation between the trapping laser beam and the coupled MT plus-end in such a system would alleviate concerns about possible photodamage to the coupling molecules, and furthermore would simplify visualization of the MT coupling site using fluorescent markers. We hope that these assays will lead to novel and exciting insights into the remarkable ability of mitotic kinetochores to undergo MT end conversion.

ACKNOWLEDGMENTS

We thank A. Korbalev for providing data for Fig. 1, and A. Zaytsev and Po-Tao Chen for critical reading of the manuscript. Funding for this work was provided by the National Institutes of Health grant GM-R01098389 to E.L.G. and American Cancer Society grant RSG-14-018-01-CCG to E.L.G. Data for Fig. 1 were obtained with support from the Russian Science Foundation (grant # 16-14-00-224).

REFERENCES

- Akiyoshi, B., Sarangapani, K. K., Powers, A. F., Nelson, C. R., Reichow, S. L., Arellano-Santoyo, H., et al. (2010). Tension directly stabilizes reconstituted kinetochore-microtubule attachments. *Nature*, *468*(7323), 576–579.
- Asbury, C. L., Gestaut, D. R., Powers, A. F., Franck, A. D., & Davis, T. N. (2006). The Dam1 kinetochore complex harnesses microtubule dynamics to produce force and movement. *Proceedings of the National Academy of Sciences of the United States of America*, *103*(26), 9873–9878.
- Bieling, P., Telley, I. A., Piehler, J., & Surrey, T. (2008). Processive kinesins require loose mechanical coupling for efficient collective motility. *EMBO Reports*, *9*(11), 1121–1127.
- Braun, M., Lansky, Z., Szuba, A., Schwarz, F. W., Mitra, A., Gao, M., et al. (2017). Changes in microtubule overlap length regulate kinesin-14-driven microtubule sliding. *Nature Chemical Biology*, *13*, 1245.
- Coue, M., Lombillo, V. A., & McIntosh, J. R. (1991). Microtubule depolymerization promotes particle and chromosome movement in vitro. *The Journal of Cell Biology*, *112*(6), 1165–1175.
- Driver, J. W., Powers, A. F., Sarangapani, K. K., Biggins, S., & Asbury, C. L. (2014). Measuring kinetochore-microtubule interaction in vitro. *Methods in Enzymology*, *540*, 321–337.
- Espeut, J., Gaussen, A., Bieling, P., Morin, V., Prieto, S., Fesquet, D., et al. (2008). Phosphorylation relieves autoinhibition of the kinetochore motor Cenp-E. *Molecular Cell*, *29*(5), 637–643.
- Grishchuk, E. L. (2017). Biophysics of microtubule end coupling at the kinetochore. *Progress in Molecular and Subcellular Biology*, *56*, 397–428.
- Grishchuk, E. L., & Ataullakhanov, F. I. (2010). In vitro assays to study the tracking of shortening microtubule ends and to measure associated forces. *Methods in Cell Biology*, *95*, 657–676.
- Grishchuk, E. L., Efremov, A. K., Volkov, V. A., Spiridonov, I. S., Gudimchuk, N., Westermann, S., et al. (2008). The Dam1 ring binds microtubules strongly enough to be a processive as well as energy-efficient coupler for chromosome motion. *Proceedings of the National Academy of Sciences of the United States of America*, *105*(40), 15423–15428.
- Grishchuk, E., McIntosh, R. J., Molodtsov, M., & Ataullakhanov, F. (2012). Force generation by dynamic microtubule polymers. In Y. E. Goldman & E. M. Ostap (Eds.), *Vol. 4. Comprehensive biophysics* (pp. 93–117). Oxford: Academic Press.
- Grishchuk, E. L., Spiridonov, I. S., Volkov, V. A., Efremov, A., Westermann, S., Drubin, D., et al. (2008). Different assemblies of the DAM1 complex follow shortening microtubules by distinct mechanisms. *Proceedings of the National Academy of Sciences of the United States of America*, *105*(19), 6918–6923.

- Gudimchuk, N., Vitre, B., Kim, Y., Kiyatkin, A., Cleveland, D. W., Ataullakhanov, F. I., et al. (2013). Kinetochore kinesin CENP-E is a processive bi-directional tracker of dynamic microtubule tips. *Nature Cell Biology*, *15*(9), 1079–1088.
- Hayden, J. H., Bowser, S. S., & Rieder, C. L. (1990). Kinetochores capture astral microtubules during chromosome attachment to the mitotic spindle: Direct visualization in live newt lung cells. *The Journal of Cell Biology*, *111*(3), 1039–1045.
- Howard, J., & Hyman, A. A. (1993). Preparation of marked microtubules for the assay of the polarity of microtubule-based motors by fluorescence microscopy. *Methods in Cell Biology*, *39*, 105–113.
- Hunt, A. J., & Howard, J. (1993). Kinesin swivels to permit microtubule movement in any direction. *Proceedings of the National Academy of Sciences of the United States of America*, *90*(24), 11653–11657.
- Hunt, A. J., & McIntosh, J. R. (1998). The dynamic behavior of individual microtubules associated with chromosomes in vitro. *Molecular Biology of the Cell*, *9*(10), 2857–2871.
- Hyman, A., Drechsel, D., Kellogg, D., Salser, S., Sawin, K., Steffen, P., et al. (1991). Preparation of modified tubulins. *Methods in Enzymology*, *196*, 478–485.
- Hyman, A. A., & Mitchison, T. J. (1991). Two different microtubule-based motor activities with opposite polarities in kinetochores. *Nature*, *351*(6323), 206–211.
- Hyman, A. A., & Mitchison, T. J. (1993). An assay for the activity of microtubule-based motors on the kinetochores of isolated Chinese hamster ovary chromosomes. In J. M. Scholey (Ed.), *Vol. 39. Methods in cell biology* (pp. 267–276): Academic Press.
- Kapoor, T. M., Lampson, M. A., Hergert, P., Cameron, L., Cimini, D., Salmon, E. D., et al. (2006). Chromosomes can congress to the metaphase plate before biorientation. *Science*, *311*(5759), 388–391.
- Kim, Y., Heuser, J. E., Waterman, C. M., & Cleveland, D. W. (2008). CENP-E combines a slow, processive motor and a flexible coiled coil to produce an essential motile kinetochore tether. *The Journal of Cell Biology*, *181*(3), 411–419.
- Koshland, D. E., Mitchison, T. J., & Kirschner, M. W. (1988). Polewards chromosome movement driven by microtubule depolymerization in vitro. *Nature*, *331*(6156), 499–504.
- Lombillo, V. A., Coue, M., & McIntosh, J. R. (1993). In vitro motility assays using microtubules tethered to Tetrahymena pellicles. *Methods in Cell Biology*, *39*, 149–165.
- Magidson, V., O’Connell, C. B., Loncarek, J., Paul, R., Mogilner, A., & Khodjakov, A. (2011). The spatial arrangement of chromosomes during prometaphase facilitates spindle assembly. *Cell*, *146*(4), 555–567.
- Maiato, H., Gomes, A. M., Sousa, F., & Barisic, M. (2017). Mechanisms of chromosome congression during mitosis. *Biology*, *6*(1), 13.
- McIntosh, J. R., Grishchuk, E. L., & West, R. R. (2002). Chromosome-microtubule interactions during mitosis. *Annual Review of Cell and Developmental Biology*, *18*, 193–219.
- McIntosh, J. R., Volkov, V., Ataullakhanov, F. I., & Grishchuk, E. L. (2010). Tubulin depolymerization may be an ancient biological motor. *Journal of Cell Science*, *123*(20), 3425–3434.
- Miller, H. P., & Wilson, L. (2010). Preparation of microtubule protein and purified tubulin from bovine brain by cycles of assembly and disassembly and phosphocellulose chromatography. *Methods in Cell Biology*, *95*, 3–15.
- Mitchison, T. J., & Kirschner, M. W. (1985). Properties of the kinetochore in vitro. II. Microtubule capture and ATP-dependent translocation. *The Journal of Cell Biology*, *101*(3), 766–777.

- Nicklas, R. B. (1983). Measurements of the force produced by the mitotic spindle in anaphase. *The Journal of Cell Biology*, *97*(2), 542–548.
- Paschal, B. M., & Vallee, R. B. (1993). Microtubule and axoneme gliding assays for force production by microtubule motor proteins. *Methods in Cell Biology*, *39*, 65–74.
- Rieder, C. L., & Salmon, E. D. (1998). The vertebrate cell kinetochore and its roles during mitosis. *Trends in Cell Biology*, *8*(8), 310–318.
- Shrestha, R. L., & Draviam, V. M. (2013). Lateral to end-on conversion of chromosome-microtubule attachment requires kinesins CENP-E and MCAK. *Current Biology*, *23*(16), 1514–1526.
- Tanaka, K., Mukae, N., Dewar, H., van Breugel, M., James, E. K., Prescott, A. R., et al. (2005). Molecular mechanisms of kinetochore capture by spindle microtubules. *Nature*, *434* (7036), 987–994.
- Tsien, R. Y. (1998). The green fluorescent protein. *Annual Review of Biochemistry*, *67*(1), 509–544.
- Volkov, V. A., Zaytsev, A. V., & Grishchuk, E. L. (2014). Preparation of segmented microtubules to study motions driven by the disassembling microtubule ends. *Journal of Visualized Experiments*, *85*, e51150. <https://doi.org/10.3791/51150>.
- Volkov, V. A., Zaytsev, A. V., Gudimchuk, N., Grissom, P. M., Gintsburg, A. L., Ataulakhanov, F. I., et al. (2013). Long tethers provide high-force coupling of the Dam1 ring to shortening microtubules. *Proceedings of the National Academy of Sciences of the United States of America*, *110*(19), 7708–7713.
- Walczak, C. E., Cai, S., & Khodjakov, A. (2010). Mechanisms of chromosome behaviour during mitosis. *Nature Reviews. Molecular Cell Biology*, *11*(2), 91–102.
- Wood, K. W., Sakowicz, R., Goldstein, L. S., & Cleveland, D. W. (1997). CENP-E is a plus end-directed kinetochore motor required for metaphase chromosome alignment. *Cell*, *91*(3), 357–366.
- Yardimci, H., van Duffelen, M., Mao, Y., Rosenfeld, S. S., & Selvin, P. R. (2008). The mitotic kinesin CENP-E is a processive transport motor. *Proceedings of the National Academy of Sciences of the United States of America*, *105*(16), 6016–6021.